SCIENTIFIC REPORTS

OPEN

SUBJECT AREAS:
ELECTRONIC PROPERTIES AND MATERIALS
ELECTRONIC DEVICES
SURFACES, INTERFACES AND THIN FILMS
ELECTRICAL AND ELECTRONIC ENGINEERING

Received
17 May 2013

Accepted
20 September 2013

Published
9 October 2013

Correspondence and requests for materials should be addressed to T.H. (hatano@riken.jp) or Y.I. (iwasa@ap.t.u-tokyo.ac.jp)

Gate Control of Electronic Phases in a Quarter-Filled Manganite

T. Hatano[1], Y. Ogimoto[1,2], N. Ogawa[1], M. Nakano[1,3], S. Ono[1,4], Y. Tomioka[5], K. Miyano[6,7], Y. Iwasa[1,8] & Y. Tokura[1,8]

[1]RIKEN Center for Emergent Matter Science (CEMS), Wako 351-0198, Japan, [2]Fuji Electric Co. Ltd., Tokyo 191-8502, Japan, [3]Institute for Materials Research, Tohoku University, Sendai 980-8577, Japan, [4]Central Research Institute of Electric Power Industry, Komae 201-8511, Japan, [5]Electronics and Photonics Research Institute, National Institute of Advanced Industrial Science and Technology (AIST), Tsukuba 305-8562, Japan, [6]Research Center for Advanced Science and Technology (RCAST), University of Tokyo, Tokyo 153-8904, Japan, [7]National Institute for Material Science (NIMS), Tsukuba 305-0047, Japan, [8]Quantum-Phase Electronics Center and Department of Applied Physics, University of Tokyo, Tokyo 113-8656, Japan.

Electron correlation often produces a variety of electrically insulating states caused by self-organization of electrons, which are particularly stable at commensurate fillings. Although collapsing such ordered states by minute external stimuli has been a key strategy toward device applications, it is difficult to access their true electronic phase boundaries due to the necessity of fine-tuning of material parameters. Here, we demonstrate the ambipolar resistance switching in $Pr_{1-x}Sr_xMnO_3$ thin films ($x = 0.5$; an effectively 1/4-filled state) by quasi-continuous control of the doping level x and band-width W using gate-voltage and magnetic field, enabled by the extreme electric-field formed at the nanoscale interface generated in an electrolyte-gated transistor. An electroresistance peak with unprecedented steepness emerges on approaching a critical point in the x-W phase diagram. The technique opens a new route to Mott-insulator based transistors and to discovering singularities hitherto unnoticed in conventional bulk studies of strongly correlated electron systems.

Control of electronic phases in a field-effect transistor (FET) configuration has been an emergent concept both for fundamental research and the development of future electronic devices[1–5]. Recent demonstrations of electric-field-induced superconductivity[6–8] and ferromagnetism[9,10] exemplify the broad applicability of an electric field of sufficient strength for phase control. In this context, the electric double-layer transistor (EDLT) plays a central role due to the extremely high electric fields attainable at the solid/liquid interface, enabling charge accumulation in the channel surface at densities as high as $10^{15}/cm^2$ (ref. 11). This is one to two orders of magnitude larger than that in conventional FETs, offering an easy access to electrostatic modulation of electronic phases. The benefits of facile and quasi-continuous control of the doping level have been clearly demonstrated in high-temperature superconductors recently[12,13]. The merit of the FET is exceptionally valuable in strongly correlated electron systems, in which the electrostatic modulation of electronic phases has attracted considerable interest because of its potential to achieve greater functionality and to realize a material-independent scaling limit[14–20]. The competition between the charge, spin and orbital degrees of freedom, gives rise to rich electronic phases, as exemplified in Mott insulators, various charge, spin and orbital orderings, multiferroics and superconductivity. At the boundary between these phases, the system is expected to be extremely sensitive to external stimuli[21–24]. In order to approach the phase boundary, one needs to control relevant parameters such as the doping level x and band-width W[23]. The tuning of x is ordinarily achieved by chemical doping whereas W is modified through chemical substitution or high pressure. However, these techniques are cumbersome and do not allow fine-tuning.

Here, we report on the search for a phase boundary in the ground-state phase diagram of the perovskite manganites $R_{1-x}A_xMnO_3$ (R = rare earth elements and A = alkaline-earth elements), where, x stands for nominal hole doping. Manganites are unique in that W can be effectively controlled by application of an external magnetic field through the double-exchange mechanism[25,26]. Among a variety of perovskite manganites, we selected $Pr_{1-x}Sr_xMnO_3$ (PSMO) in the vicinity of $x \sim 0.5$ corresponding to the 1/4-filled state[27,28]. The phase diagram of bulk materials at $B = 0$ T is known to be very rich as shown in Fig. 1a. Upon hole doping, the ground-state evolves from a ferromagnetic metal (FM) to an A-type antiferromagnetic insulator (A-AFI) near $x = 0.5$, where the phase boundary is very sensitive to the hole doping. Quasi-continuous scans of both x and W, by means of EDLT and magnetic field, respectively, enabled us to uncover an insulating state in an extremely narrow range

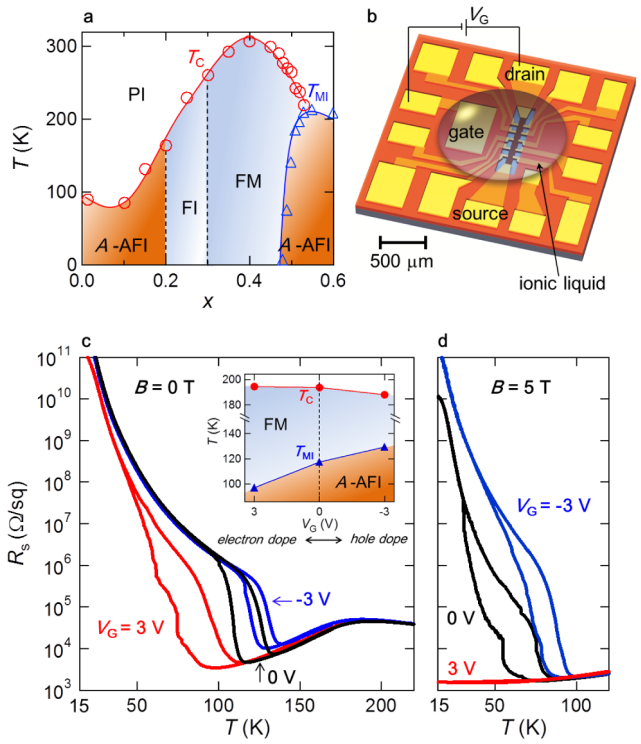

Figure 1 | The electric-field effect on the transport properties of a 5 nm-thick $Pr_{1-x}Sr_xMnO_3$ (PSMO) thin film. (a), The electronic phase diagram of bulk PSMO with varying doping level $0.0 < x < 0.6$. PI, *A*-AFI, FI and FM, denote paramagnetic insulator, *A*-type antiferromagnetic insulator, ferromagnetic insulator and ferromagnetic metal, respectively. Open red circles and blue triangles indicate Curie temperature (T_C) and the metal-insulator transition temperature (T_{MI}), respectively. (b), Schematic diagram of the electric double layer transistor with an ionic liquid electrolyte. (c), The temperature (T) dependence of the sheet resistance (R_s) at gate voltage (V_G) of 0 and ±3 V. The positive and negative V_G correspond to electron and hole doping, respectively. The inset shows gate voltage dependence of both T_C and T_{MI} defined as the temperature where $d(\log R_s)/dT = 0$ on cooling. (d), R_s-T curves of the device at the magnetic field (B) of 5 T for $V_G = 0$ and ±3 V.

of carrier density (vide infra). Utilizing this critical phase, an ambipolar phase control by gate voltage (V_G) was realized in the strongly correlated electron system, demonstrating the importance of field-effect phase control in the search for new states and functions of matter.

Results

The sample was a PSMO epitaxial thin film prepared by a pulsed-laser deposition method. It was patterned into a Hall-bar structure and both the channel and the gate electrode were covered by the ionic liquid for the application of electric fields (Fig. 1b). We examined the V_G dependence of sheet resistance (R_s) vs. temperature (T) curves for a 5 nm-thick PSMO film, as shown in Fig. 1c. At $V_G = 0$ V, the R_s showed an appreciable decrease below the Curie temperature (T_C) of 193 K, followed by a sharp metal-insulator (MI) transition at the transition temperature (T_{MI}) of 117 K in a cooling process. The temperature hysteresis was rather reproducible, indicating that it is originated from quenched disorder such as defects existing in the channel. With a positive bias of $V_G = 3$ V, corresponding to electron doping, T_{MI} decreased to 96 K, whereas T_C slightly increased to 195 K. For hole doping with a negative bias of $V_G = -3$ V, T_{MI} increased to 130 K and T_C decreased to 187 K. Thus, T_{MI} shifted by 30 K through gating of $V_G = -3$ V to 3 V as summarized in the inset of Fig. 1c, which quantitatively agrees with an expanded phase diagram of chemically doped PSMO around $x \sim 0.5$. Note that the device performance was highly reversible against repeated application of V_G, and was also reproducible in different devices as shown in Supplementary Information.

To investigate the effect of W modulation, we measured the gate effects under a magnetic field of $B = 5$ T as shown in Fig. 1d. Owing to the enhanced W by the magnetic field, $V_G = 3$ V was strong enough to completely suppress the insulating state observed below T_{MI} of ~60 K at $V_G = 0$ V. In contrast, the negative gate voltage of $V_G = -3$ V increased T_{MI} to ~80 K and increased R_s below T_{MI} concomitantly. Application of magnetic field made the R_s-T curve much more sensitive to V_G. The colossal electroresistance was as large as eight orders of magnitude at 20 K. A further increase of W ($B = 7.5$ T) revealed an unexpected V_G dependence of R_s as displayed in Fig. 2a. The insulating behavior at $T = 20$ K was already suppressed even at $V_G = 0$ V, and the FM state was realized by applying only $V_G = 1$ V. As V_G was swept to negative, R_s at low temperature started to increase, reached a maximum at $V_G = -1.4$ V, and then decreased, showing '*ambipolar*' device operation. This indicates that hole doping also stabilized a metallic state although R_s below T_{MI} was not as low as that in the electron doped state. This behavior is clearly illustrated in a three-dimensional plot of R_s in the V_G-T plane as shown in Fig. 2b. There is a peculiar singular point, where an insulating state is stabilized in a very narrow V_G region near −1.4 V. A V_G sweep of ~±50 mV results in a four orders of magnitude change in R_s. This gigantic and steep ambipolar behavior suggests that $V_G = -1.4$ V corresponds to the exactly 1/4-filled state ($x = 0.5$), as will be discussed below. Naturally, it is highly unlikely that the exactly 1/4-filled state will be realized to this level of accuracy by chemical means and thus it must have escaped our observation thus far. Note that this critical feature reproduces even in other devices (see Supplementary Information).

Discussion

To understand the singular behavior at $V_G = -1.4$ V, we explored the V_G dependence of the R_s-T curve while varying the magnetic field strength. Figure 2c displays pseudo-color plots of R_s in the V_G-T plane for $B = 5$–8 T. At $B = 5$ T, the AFI state (the red-to-green colored region) rises from $V_G = 1.5$ V toward the negative V_G region, showing no anomaly at $V_G = -1.4$ V, i.e., at the exactly 1/4-filled state. With increasing W, the FM state (the blue colored region) becomes dominant not only at the electron doping side ($V_G > -1.4$ V) but also at the hole doping side ($V_G < -1.4$ V) with the appearance of a robust insulating phase only at $V_G = -1.4$ V, which clearly stands out above 7 T. Note that R_s at the hole side is higher than that at the electron side. Figure 3a highlights this anomaly at $V_G = -1.4$ V, where we plot R_s at 20 K in the V_G-B plane, equivalent to a phase diagram in x-W coordinates. Although the overall trend in Fig. 3a is metallization on increasing W, the insulating state at the 1/4-filling robustly remains on the narrow region of ~±50 mV at $B = 7.5$ T. By passing over this sharp insulating phase, one should expect the gate-induced conversion from the insulating state to conducting states only by infinitesimal voltages. This would lead to the new concept of low-power-consumption and steep switching devices rather exceeding conventional FETs.

The singular nature of the insulating phase at $V_G \sim -1.4$ V, which penetrates deep into the wider W region (shown in Fig. 3a), indicates that its origin differs from that for the broader insulating phase seen in smaller W. Based on the x-W phase diagram (shown in Fig. 3b), we attribute the stable insulating phase only at the 1/4-filling to the charge/orbital ordered (COO) state, whereas the broader insulating state away from the 1/4-filled state is ascribed to the *A*-AFI. Figure 3b shows a schematic phase diagram in terms of x and W in the vicinity of $x \sim 0.5$, proposed for bulk perovskite manganite compounds at zero magnetic field[29]. The chemical composition corresponding to

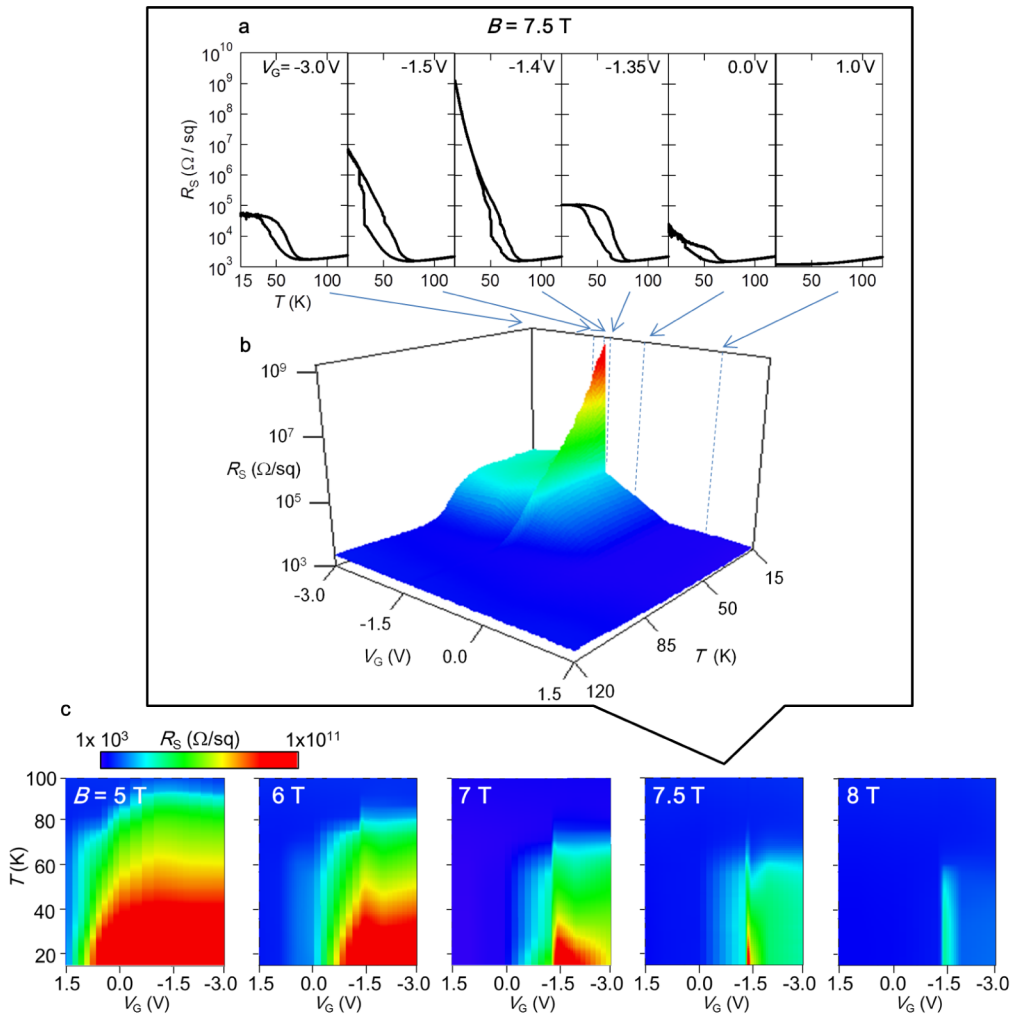

Figure 2 | A robust insulating state confined in a very narrow gate voltage region.(a), The temperature dependence of R_s at different V_G ranging from −3 V to 1 V under $B = 7.5$ T. (b), A three-dimensional plot of R_s measured in a warming process under $B = 7.5$ T as functions of temperature and V_G. (c), Contour plots of R_s on the T-V_G plane at various magnetic fields from $B = 5$ T to 8 T. These plots correspond to electronic phase diagrams under magnetic fields in the vicinity of $x = 0.5$. Note that the direction of abscissa is taken to facilitate the comparison of V_G with x in the phase diagram, Fig. 1a. See also Fig. 3a below.

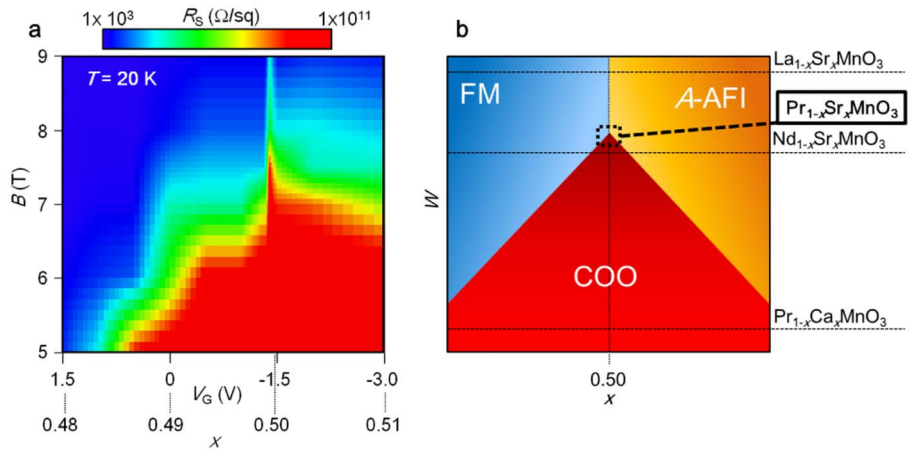

Figure 3 | The ground-state phase diagram of PSMO.(a), Contour plot of Rs on the V_G-B plane at $T = 20$ K showing the ground state phase diagram in the doping level x - band width W plane. A change in V_G by ±1.5 V corresponds to a change in x of ±0.01 as estimated by the electrostatic carrier accumulation with a capacitance of 10 μF/cm² (ref. 11). (b), A schematic of a metal-insulator phase diagram of perovskite manganites in the plane of x and W. A rectangle with dashed line located around $x \sim 0.5$ indicates the scan area shown in Fig. 3a. COO denotes charge/orbital ordered insulating phase.

the particular value of W is shown on the right side. As prototypical materials, $La_{1-x}Sr_xMnO_3$ and $Pr_{1-x}Ca_xMnO_3$ are well known for having large and small W, respectively[30,31]. While the latter exhibits very wide COO phase, it is much reduced in $Nd_{1-x}Sr_xMnO_3$ with a larger W, as shown in Fig. 3b. With a yet larger W, PSMO has been considered to be located just around the critical point, at which three phases compete[29]. However, by comparing Figs. 3a and 3b, we are compelled to ascribe that the COO state is anomalously stabilized extending deep into the larger W at the exact 1/4 filling. Therefore, the scanned region of our experiment shown in Fig. 3a lies within the rectangle delineated by dashed lines in Fig. 3b. The robustness of the COO phase arises from the commensurability of the 1/4-filling. i.e., one e_g electron per two Mn sites. This phenomenon has escaped our detection in the past because R_s in the A-AFI state under ordinary circumstances is too high to distinguish it from COO in simple transport measurements and because the exact filling condition is too severe to be achieved by chance. Indeed, the width of COO state in the doping level, i.e. the doping modulation (Δx) in the ± 50 mV sweeping of V_G, is roughly estimated as $\Delta x \sim \pm 0.0004$ by assuming the penetration of accumulated carriers into the whole 5 nm-thick film (see Supplementary Information). The narrow range of $\Delta x \sim \pm 0.0004$ in PSMO together with the fact that it stands out only near a particular W would cause serious difficulties in chemical approach. This is the reason why the existence of the COO in bulk PSMO single crystals is still in debate[29,32,33]. The nature of the robust insulating state at the 1/4-filling is left to be clarified by in-situ neutron and x-ray scattering studies.

In summary, we demonstrate the gate-induced ambipolar phase switching associated with the colossal electroresistance in transistor devices of 1/4-filled PSMO by using a combination of external electric and magnetic fields. Quasi-continuous parameter control allowed us to map out the ground-state phase diagram of PSMO near a critical point, where we found a stable insulating state existing in a very narrow region of $\Delta x = \pm 0.0004$, which could be collapsed by a small voltage of ± 50 mV generating a gigantic responses in R_s. More generally, our results revealed that a relatively small carrier modulation of $\pm 10^{19}/cm^3$, corresponding to $\Delta x = \pm 0.0004$, has a tremendous impact on a correlated electron system containing more than $10^{22}/cm^3$ order of carriers. Such a gigantic response and a buried state at the critical point should not be peculiar to perovskite manganites alone, but should be common to strongly correlated electron systems, offering a novel opportunity to construct phase transition FET devices that operate with quite a low voltage.

Methods

The epitaxial thin film of PSMO was grown on a (110)-oriented $(LaAlO_3)_{0.3} - (SrAl_{0.5}Ta_{0.5}O_3)_{0.7}$ substrate by a pulsed-laser deposition method (+0.7% mismatch). The film is coherently grown, i.e., the in-plane lattice is clamped to the substrate. Here the use of the (110)-oriented substrate allowed the Jahn-Teller distortion in the film required for the first-order phase transition and enabled us to observe a sharp metal-insulator transition even in ultra-thin films[28,34]. The film was patterned into a Hall-bar structure with a side gate located in the vicinity of channel by photo-lithography and Ar-ion milling. The channel was 520 μm long and 30 μm wide. All Au electrodes were deposited by electron-beam evaporation. Prior to this evaporation, we treated the film surface with O_2 plasma for enhancing the Au adhesion. A hard-baked photoresist was used for electrical isolation between the side gate and channel. We completed the device by putting a small amount of ionic liquid N,N-diethyl-N-(2-methoxyethyl)-N-methylammonium bis-trifluoromethylsulfonyl)-imide on the channel and side gate. We measured R_s with a standard four-probe configuration by applying V_G using a semiconductor parameter analyzer. Temperature was swept from 220 K to 15 K at a cooling/heating rate of 2.5 K/min. We applied V_G at 220 K and kept it until the gate current was saturated before starting temperature sweep.

1. Ahn, C. H. *et al.* Electrostatic modification of novel materials. *Rev. Mod. Phys.* **78**, 1185–1212 (2006).
2. Glover, R. E. & Sherrill, M. D. Changes in superconducting critical temperature produced by electrostatic charging. *Phys. Rev. Lett.* **5**, 248–250 (1960).
3. Mathews, S., Ramesh, R., Venkatesan, T. & Benedetto, J. Ferroelectric field effect transistor based on epitaxial perovskite heterostructures. *Science* **276**, 238–240 (1997).
4. de Boer, R. W. I., Gershenson, M. E., Morpurgo, A. F. & Podzorov, V. Organic single-crystal field-effect transistors. *phys. stat. sol.* (a) **201**, 1302–1331 (2004).
5. Ahn, C. H. *et al.* Electrostatic modulation of superconductivity in ultrathin $GdBa_2Cu_3O_{7-x}$. *Science* **284**, 1152–1155 (1999).
6. Ueno, K. *et al.* Electric-field-induced superconductivity in an insulator. *Nature Mater.* **7**, 855–858 (2008).
7. Ye, J. T. *et al.* Liquid-gated interface superconductivity on an atomically flat film. *Nature Mater.* **9**, 125–128 (2009).
8. Ueno, K. *et al.* Discovery of superconductivity in $KTaO_3$ by electrostatic carrier doping. *Nature Nanotechnol.* **6**, 408–412 (2011).
9. Ohno, H. *et al.* Electric-field control of ferromagnetism. *Nature* **408**, 944–946 (2000).
10. Yamada, Y. *et al.* Electrically induced ferromagnetism at room temperature in cobalt-doped titanium dioxide. *Science* **332**, 1065–1067 (2011).
11. Yuan, H. T. *et al.* High-density carrier accumulation in ZnO field-effect transistors gated by electric double layers of ionic liquids. *Adv. Funct. Mater.* **19**, 1046–1053 (2009).
12. Bollinger, A. T. *et al.* Superconductor-insulator transition in $La_{2-x}Sr_xCuO_4$ at the pair quantum resistance. *Nature* **472**, 458–460 (2011).
13. Leng, X., Barriocanal, J. G., Bose, S., Lee, Y. & Goldman, A. M. Electrostatic control of the evolution from a superconducting phase to an insulating phase in ultrathin $YBa_2Cu_3O_{7-x}$ films. *Phys. Rev. Lett.* **107**, 027001 (2011).
14. Zhou, C., Newns, D. M., Misewich, J. A. & Pattnaik, P. C. A field effect transistor based on the Mott transition in a molecular layer. *Appl. Phys. Lett.* **70**, 598–600 (1997).
15. Newns, D. M. *et al.* Mott transition field effect transistor. *Appl. Phys. Lett.* **73**, 780–782 (1998).
16. Asanuma, S. *et al.* Tuning of the metal-insulator transitions in electrolyte-gated $NdNiO_3$ thin films. *Appl. Phys. Lett.* **97**, 142110 (2010).
17. Scherwitzl, R. *et al.* Electric-field control of the metal-insulator transition in ultrathin $NdNiO_3$ films. *Adv. Mater.* **22**, 5517–5520 (2010).
18. Dhoot, A. S., Israel, C., Moya, X., Mathur, N. D. & Friend, R. H. Large electric field effect in electrolyte-gated manganites. *Phys. Rev. Lett.* **102**, 136402 (2009).
19. Xiang, P. H. *et al.* Strain-mediated phase control and electrolyte-gating of electron-doped manganites. *Adv. Mater.* **23**, 5822–5827 (2011).
20. Nakano, M. *et al.* Collective bulk carrier delocalization driven by electrostatic surface charge accumulation. *Nature* **487**, 459–462 (2012).
21. Mott, N. F. *Metal-Insulator Transitions* (Taylor & Francis, London, 1990).
22. Tokura, Y. *Colossal Magnetoresistive Oxides* (Gordon & Breach Science Publishers, 2000).
23. Imada, M., Fujimori, A. & Tokura, Y. Metal-insulator transitions. *Rev. Mod. Phys.* **70**, 1039–1263 (1998).
24. Lee, H. S., Choi, S. G., Park, H. & Rozenberg, M. J. A new route to the Mott-Hubbard metal-insulator transition: Strong correlations effects in $Pr_{0.7}Ca_{0.3}MnO_3$. *Sci. Rep.* **3**, 1704 (2013).
25. Zener, C. Interaction between the d-Shells in the Transition Metals. II. Ferromagnetic Compounds of Manganese with Perovskite Structure. *Phys. Rev.* **86**, 403 (1951).
26. Kuwahara, H., Tomioka, Y., Asamitsu, A., Moritomo, Y. & Tokura, Y. A first-order phase transition induced by a magnetic field. *Science* **270**, 961–963 (1995).
27. Knizek, K., Jirak, Z., Pollert, E., Zounova, F. & Vratislav, S. Structure and magnetic properties of $Pr_{1-x}Sr_xMnO_3$ perovskites. *J. Solid State Chem.***100**, 292–300 (1992).
28. Ogimoto, Y. *et al.* Pseudomorphic strain effect on the charge-orbital ordering pattern in $Pr_{0.5}Sr_{0.5}MnO_3$ epitaxial thin films. *Appl. Phys. Lett.* **86**, 112513 (2005).
29. Kajimoto, R., Yoshizawa, H., Tomioka, Y. & Tokura, Y. Stripe-type charge ordering in the metallic A-type antiferromagnet $Pr_{0.5}Sr_{0.5}MnO_3$. *Phys. Rev. B* **66**, 180402 (2002).
30. Hemberger, J. *et al.* Structural, magnetic and electrical properties of single-crystalline $La_{1-x}Sr_xMnO_3$ ($0.4 < x < 0.85$). *Phys. Rev. B* **66**, 094410 (2002).
31. Jirak, Z., Krupicka, S., Simsa, Z., Dlouha, M. & Vratislav, S. Neutron diffraction study of $Pr_{1-x}Ca_xMnO_3$ perovskites. *J. Magn. Magn. Mater.* **53**, 153–166 (1985).
32. Tomioka, Y., Asamitsu, A., Moritomo, Y., Kuwahara, H. & Tokura, Y. Collapse of a charge-ordered state under a magnetic field in $Pr_{1/2}Sr_{1/2}MnO_3$. *Phys. Rev. Lett.* **74**, 5108–5111 (1995).
33. Kawano, H. *et al.* Magnetic ordering and relation to the metal-insulator transition in $Pr_{1-x}Sr_xMnO_3$ and $Nd_{1-x}Sr_xMnO_3$ with $x \sim 1/2$. *Phys. Rev. Lett.* **78**, 4253–4256 (1997).
34. Nakamura, M., Ogimoto, Y., Tamaru, H., Izumi, M. & Miyano, K. Phase control through anisotropic strain in $Nd_{0.5}Sr_{0.5}MnO_3$ thin films. *Appl. Phys. Lett.* **86**, 182504 (2005).

Acknowledgments

We are grateful to M. Nakamura and Y. Tokunaga for fruitful discussions. This research was supported by the Japan Society for the Promotion of Science (JSPS) through its "Funding Program for World-Leading Innovative R&D on Science and Technology (FIRST Program)", initiated by the Council for Science and Technology Policy (CSTP), and by JSPS Grant-in-Aid for Scientific Research No. 24224009, No. 25000003 and No. 25708040. T.H. and M.N. were supported by RIKEN through the Incentive Research Grant. Y.I. was

supported by Strategic International Collaborative Research Program (SICORP, LEMSUPER) from Japan Science and Technology Agency (JST).

Author contributions

T.H. fabricated the devices, performed the measurements, and analyzed the data. Y.O. and N.O. grew the films. M.N. and S.O. contributed to the device fabrications and experimental set-up. T.H., Y.O., K.M., Y.I. and Y.T. planned and supervised the study. T.H., Y.O., M.N., K.M., Y.I. and Y.T. wrote the manuscript. All authors discussed the results and commented on the manuscript.

Additional information

Supplementary information accompanies this paper at http://www.nature.com/scientificreports

Competing financial interests: The authors declare no competing financial interests.

How to cite this article: Hatano, T. *et al.* Gate Control of Electronic Phases in a Quarter-Filled Manganite. *Sci. Rep.* **3**, 2904; DOI:10.1038/srep02904 (2013).